BNL-NUREG-64175
CONF-970826--5

FINITE ELEMENT ANALYSES FOR SEISMIC SHEAR WALL INTERNATIONAL STANDARD PROBLEM

Y. Park, C. Hofmayer
Brookhaven National Laboratory, Upton, NY USA

N. Chokshi
U.S. Nuclear Regulatory Commission, Washington, DC USA

ABSTRACT

This paper presents an overview of the state-of-the-art on the application of nonlinear FEM analysis to RC shear wall structures under severe earthquake loadings based on the findings obtained during the SSWISP Workshop in 1996. Also, BNL's analysis results of the ISP shear walls under monotonic static, cyclic static and dynamic loading conditions are described.

1 INTRODUCTION

The finite element method (FEM) is now widely used as a practical structural design tool to analyze complex structures in both the nuclear and non-nuclear industries. In the seismic design of shear wall structures, e.g., nuclear reactor buildings, a linear FEM analysis is frequently used to quantify the stresses under the design loading condition. The final design decisions, however, are still based on empirical design rules established over decades from accumulated laboratory test data.

Over the last two decades, the application of nonlinear FEM to reinforced concrete (RC) structures has been considered an alternate analysis/design tool for seismic structural design. In recent years, significant improvements have been made in Europe, Japan and the United States in both the numerical techniques and the development of constitutive model for concrete. However, it has been recognized that further improvements in the analysis methods are needed, particularly in the area where highly plastic loading reversals are involved (Ref. 1). The Seismic Shear Wall International Standard Problem (SSWISP) offered a unique opportunity to perform state-of-the-art nonlinear dynamic analyses of shear wall structures under earthquake loadings, as well as to collect information on the currently available analysis methods worldwide.

The Nuclear Power Engineering Corporation (NUPEC) of Japan offered the dynamic test results of shear wall structures to the OECD/NEA/CSNI (Organization for Economic Corporation and Development/Nuclear Energy Agency/Committee on the Safety of Nuclear Installation) for use as an International Standard Program (ISP). Two identical shear walls, which consisted of a web, flanges, and massive top and bottom slabs, were tested to ultimate failure under earthquake motions at NUPEC's Tadotsu Engineering Laboratory. The shear walls simulated a part of a typical reactor building.

The test results and detailed information on the test conditions were made available by NUPEC, and the participants in the SSWISP were asked to perform structural analyses to reproduce the test results. During the SSWISP Workshop at Yokohama, Japan in May 1996, a total of 55 analyses were presented by 30 participants from 11 different countries (Ref. 2). Several participants presented remarkable nonlinear dynamic analysis results using originally developed in-house codes, which were considered to be at various stages of developments.

This paper presents an overview of the state-of-the-art on the application of nonlinear FEM analyses to RC shear wall structures based on the findings obtained during the SSWISP, and also summarizes BNL's analysis results.

2 OVERVIEW OF STATE-OF-THE-ART OF ANALYSIS METHODS

Constitutive Models of Concrete. . . . .Under severe earthquake loadings, concrete undergoes repeated crack opening/closings as well as compression softening with the principal stress directions constantly rotating. Many of the participants of the SSWISP Workshop experienced technical difficulties in developing a reliable constitutive model for the ISP shear walls that were subjected to highly plastic dynamic loading reversals. Some elements in the constitutive model of concrete, which are considered to play key roles in successful analyses, are listed in Table 1, and discussed below.

Table 1 Key Elements in Constitutive Models of Concrete

Key Elements	Popular Modeling in Successful Analyses
Basic Plasticity Formulation	Orthotropic Plasticity with Equivalent Uniaxial Stress-Strain Concept
Hysteretic Model for Concrete	Compression and tension softening and realistic/detailed unloading/reloading curves
Compressive Strength Reduction	Vecchio-Collins/Noguchi models
Shear Retention Factor	Yamada-Aoyagi/Maekawa models
Crack Control	Rotating smeared crack model

For the basic plasticity formulation to define the so-called D-matrix for concrete, two approaches are widely used, i.e., modified classical plasticity theories (e.g., Ref. 3) and the orthotropic plasticity theory based on the equivalent uniaxial stress-strain concept (e.g., Ref. 4). It seems the latter method is becoming increasingly popular as the complex uniaxial stress-strain relationship of concrete can be more directly incorporated in the model. In most past studies, efforts were made to make the D-matrix symmetric such as by manipulating the definition of Poisson's ratio. However, it is being increasingly recognized that the D-matrix for cracked concrete should be non-symmetric in nature (e.g., Ref. 6), and there are no significant computational advantages in using a symmetric matrix over a non-symmetric matrix.

As an example for the uniaxial stress-strain relationship of concrete, Figure 1 illustrates the hysteretic model used in BNL's analysis described later. In formulating such a hysteretic model and implementing it in an FEM computer code, considerations should be given to two aspects; i.e., the unique hysteretic behavior of concrete under cyclic strain reversals, and a numerical instability in solutions caused by abrupt changes in stiffness values. The unique features of concrete that need to be included in a hysteretic model may include:

- Negative slope in both tension and compression sides to account for tension and compression softenings;
- Strength and stiffness deteriorations due to cycling on the compression side;
- Hysteretic damping in unloading/reloading path;
- Multi-linear or curved lines for unloading path on the compression side.

Regarding the numerical instability problem, it should be recognized that an abrupt change in stiffness values as well as repeated artificial unloading/reloadings during numerical iterations can be a main cause of erroneous analysis results for cyclic/dynamic loading applications. In order to avoid this problem, hysteretic paths, particularly for those of smaller unloading/reloading paths, should be made as smooth as possible as illustrated in Figure 1. Alternatively, a simplified hysteretic model, such as illustrated in Figure 2, can be used to minimize the numerical problems. Several analysis results using such a simplified model (Ref. 2) indicate that analysis could reasonably reproduce moderately nonlinear dynamic responses, but failed to duplicate highly plastic responses. Also, an additional damping should be considered in dynamic analysis using such a simplified hysteretic model to compensate for the lack of hysteretic damping in unloading/reloading paths.

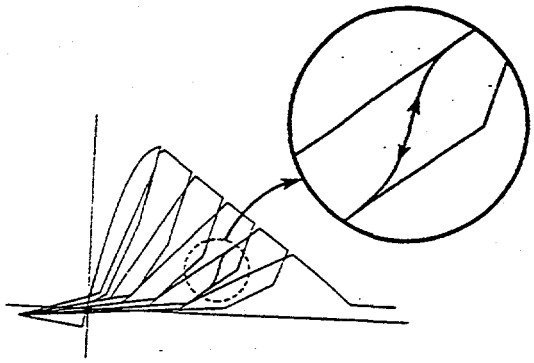

Figure 1 Uniaxial Hysteretic Model for Concrete

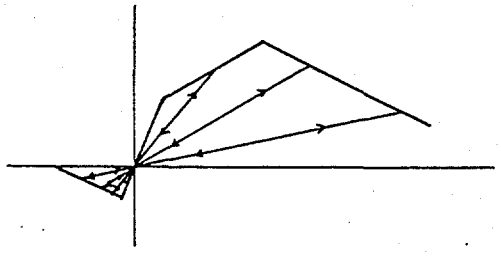

Figure 2 Simplified Hysteretic Model

Since the early 1980's, it has been recognized that the compressive strength in the direction parallel to the cracks of cracked concrete tends to be lower than the uniaxial compressive strength, f'_c. How to quantify this compressive strength reduction is still a matter of controversy due to a large scatter observed for this factor. Empirical formulations developed by Vecchio and Collins (Ref. 7) and by Noguchi et. al. (Ref. 8) are widely used in recent studies. According to Vecchio and Collins (1992), the reduction factor, β, is expressed by the ratio of the tensile principal strain, ϵ_1, to the compressive principal strain, ϵ_3, in a triaxial stress condition as,

$$\beta = \frac{1}{1+K_s K_f}, \quad K_s = 0.35\left(-\frac{\epsilon_1}{\epsilon_3} - 0.28\right)^{0.8}, \quad K_f = 0.1825\sqrt{f'_c} \tag{1}$$

and f'_c is expressed in MPa. Noguchi's formulation is somewhat similar as,

$$\beta = \frac{1}{0.27 + 0.96\ (\epsilon_t/\epsilon_o)^{0.167}} \tag{2}$$

in which, ϵ_t is the average tensile strain, and ϵ_o is the strain at the uniaxial compressive strength. Based on the author's experience, the implementation of the above Equation 1 in an FEM code is difficult as the ratio, ϵ_1/ϵ_3, tends to vary wildly under cyclic loading conditions. For this reason, the following older version of Vecchio and Collins equation seems to be used more frequently;

$$\beta = \frac{1}{1 + 0.27\ (\epsilon_t/\epsilon_o - 0.37)} \tag{3}$$

The shear retention of cracked concrete due to aggregate interlocking is considered to have a greater influence on the analysis results than the foregoing strength reduction factor. A large number of models to account for this factor have been proposed in the past. Among simpler models, the following Yamada-Aoyagi model is probably the most popular choice due to the ease in programming implementation. The shear modulus, G, is expressed as a function of the elastic shear modulus, G_o, and the maximum tensile strain, ϵ_{max}, as

$$G\ (kg/cm^2) = \frac{1}{\frac{1}{G_o} + \frac{\epsilon_{max}}{36}} \tag{4}$$

Another popular simplified/practical approach is to express the inelastic shear modulus as a function of the equivalent uniaxial moduli, E_i, and Poisson's ratio, ν, based on the orthotropic plasticity theory, such as for a biaxial stress condition,

$$G = \frac{1}{4(1+\nu)}\ (E_1 + E_2) \tag{5}$$

It should be pointed out that these formulations are not supported by experimental verifications, and tend to overestimate the shear retention.

As experimental results on the shear transfer across a cracked surface have become more available (e.g., Refs. 9 and 10), more sophisticated models have been proposed in which an independent hysteretic model is constructed for the transferred shear-crack slippage relation, and the strength and stiffness parameters are expressed as a function of the tensile strain normal to the crack surface, ϵ_t. For example, according to Ref. 9, the envelope curve for such a hysteretic model is,

$$\tau(MPa) = 3.83 f'^{1/3}_c \frac{(\gamma/\epsilon_t)^2}{1 + (\gamma/\epsilon_t)^2} \quad (6)$$

in which, τ is the transferred shear; and γ is the shear strain per crack width.

The use of such a sophisticated model in cyclic/dynamic analyses may not be straightforward due to a numerical instability problem, particularly when the concrete element enters the compressive negative slope region.

The so-called rotating smeared crack model is widely used to control the crack opening/closing under cyclic loading reversals. In this model, the angle of the principal stress direction, θp, is allowed to rotate freely for virgin concrete until cracking occurs. While a crack is opening the θp is fixed, and starts to rotate again after the closing of the crack. Since the stress states of concrete are highly sensitive to a small change in the θp, additional considerations in programming are needed to avoid abrupt changes in θp.

Numerical Procedures. . . . .Most of the currently available FEM codes are limited to monotonic push-over type loading conditions for the nonlinear analysis of concrete structures. Significant technical difficulties exist in expanding these codes to treat cyclic/dynamic loading conditions. Some of the numerical problems and possible solutions are listed in Table 2 based on the author's experience as well as findings obtained from the SSWISP Workshop.

The numerical problems associated with unbalanced forces (mismatch of element internal forces) are usually much more serious in the analysis of RC structures than most other types of nonlinear analyses because of abrupt stiffness changes caused by cracking and crushing of concrete. Figures 3(a) through (c) illustrate typical numerical algorithms used in most nonlinear FEM codes, i.e., Newton-Raphson (N-R), modified Newton-Raphson (modified N-R), and initial stiffness methods. To suppress the unbalanced forces under a sufficiently low level, a combination of some of these methods is considered to be more effective. For instance, in BNL's analyses described later, all the foregoing three iteration schemes, i.e., N-R, modified N-R and initial stiffness methods, are used in succession for each analysis step.

Table 2 Numerical Problems Associated with Analysis for Cyclic/Dynamic Loads

Numerical Problems	Possible Solutions
Unbalanced forces	Combined iteration scheme
Stability at Negative slope	Sub-stepping option
Interaction of Solvers with Constitutive model	Smooth changes in material parameters
Numerical ratcheting	Minimize number of numerical iterations
Instability in acceleration response (in dynamic analysis)	Use of linear internal damping

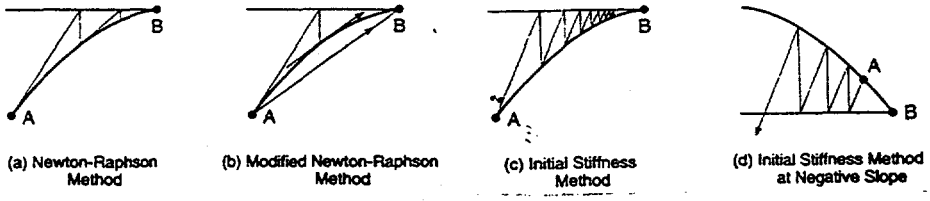

Figure 3 Numerical Algorithms for Nonlinear Analysis (analysis step is from point-A to point-B)

The numerical stability of the analysis solutions will rapidly deteriorate when the analysis model enters a negative slope region such as due to a brittle shear failure. Once the model structure starts to reduce its resistance forces at an increased deformation, the foregoing unbalanced forces tend to accumulate faster, and the repeated applications of the initial stiffness method may aggravate the solutions, rather than improve them, as illustrated in Figure 3(d). The so-called sub-stepping option together with minimum number of iterations would be a practical solution. In this approach, an analysis increment is further sub-divided, thereby significantly reducing the size of unbalanced forces for each analysis step.

The numerical problems caused by the interaction between the numerical solver and material constitutive model are highly complex phenomena, and sometimes it is difficult to identify the root cause of the problem. Abrupt changes in material parameters, e.g., stiffnesses, Poisson's ratio and biaxial interaction factors, may sometimes cause numerical oscillations during numerical iterations, and that in turn may cause repeated artificial unloading/reloading in the material model. An effort needs to be made to make the transition of all the material parameters as smooth as possible in programming implementation.

The phenomenon, "numerical ratcheting", is not unique to the nonlinear FEM analysis of RC structures. In the area of piping stress analysis, a number of studies have found that most of the existing nonlinear FEM codes tend to overpredict the accumulation of plastic strains (i.e., ratcheting) for pipe elbows under repeated cyclic loads (e.g., Ref. 11). During the iteration phase of calculations, most analysis codes repeatedly apply static nodal forces to reduce the unbalanced forces. This tends to push the model in the weaker (softer) direction, and thereby causing a numerical ratcheting. The only known measure so far is to minimize the number of iterations, which will reduce the amount of numerical ratcheting, but will not eliminate it.

In dynamic analyses, the external forces, which are used to evaluate the unbalanced forces, are calculated from acceleration responses. This is a potential cause of additional numerical difficulties in nonlinear dynamic analyses since the unbalanced forces are calculated by subtracting one response quantity (internal forces) from another (acceleration responses). In nonlinear dynamic analysis, in general, acceleration responses are very sensitive to stiffness changes. An abrupt change in material parameters will cause acceleration pulses, which is translated into erroneous unbalanced forces, and feedback into the analysis model. As a result, a high frequency component is introduced in the dynamic responses, which may cause a serious numerical problem. One practical measure to suppress this high frequency component is the use of linear internal damping, i.e., a Rayleigh damping which is proportional to the elastic stiffness matrix.

3 SSWISP SHEAR WALL TEST

Figure 4 shows the tested shear wall, which consisted of a web (3 meters wide, 75 mm thick, and 2.02 meters high), flanges (2.98 meter wide, 100 mm thick and 2.02 meters high), and massive top (122 tonf) and bottom slabs. The reinforcement ratio is 1.2% for both web and flanges in both the horizontal and vertical directions. The material properties are summarized in Table 3.

Two identical shear walls were tested at six amplitude levels, starting from the lower elastic run to the ultimate failure. The recorded peak responses are summarized in Figure 5 in terms of the maximum inertia forces and the top horizontal displacements. During the highest amplitude test run, the shear wall failed catastrophically due to a sudden sliding shear failure.

Table 3 Material Properties

Rebars	Concrete
Yield Stress, fy = 39.1 kg/mm^2 M. of Elasticity, E = 18.8 x 10^3 kg/mm^2 Tensile Strength, f_u = 49.5 kg/mm^2	Compressive Strength, f'$_c$ = 2.92 kg/mm^2 M. of Elasticity, E = 23.4 kg/mm^2 Poisson's ratio, ν = 0.155 Tensile strength, f_t = 0.23 kg/mm^2

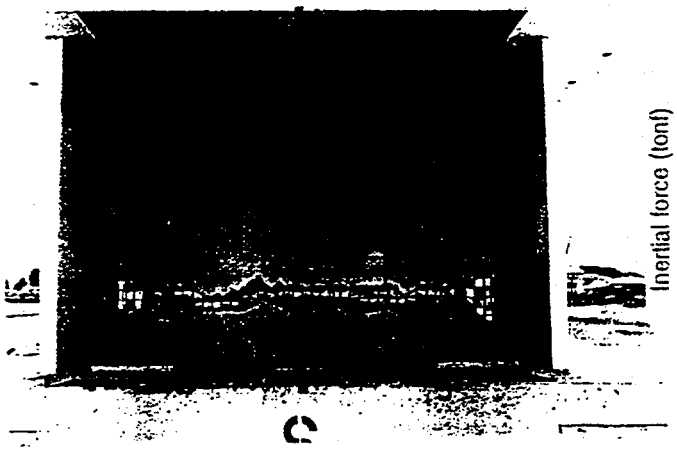

Figure 4 ISP Shear Wall After Tests

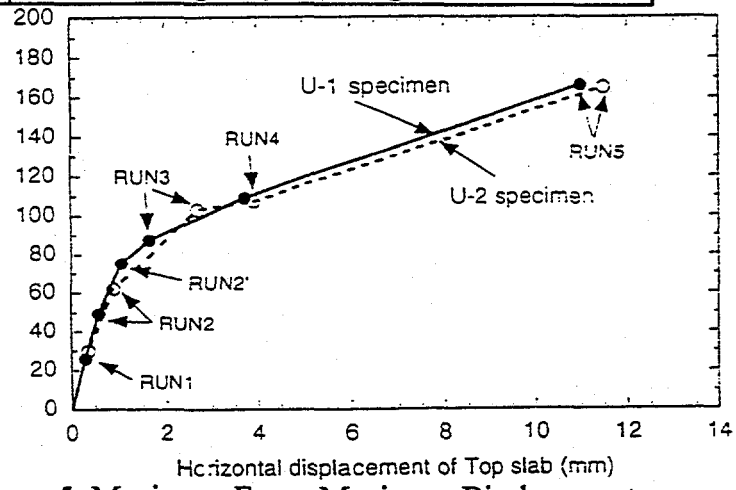

Figure 5 Maximum Force-Maximum Displacement Relationship

4 ANALYSIS METHOD

Figure 6 shows the analysis model used by BNL. Simple 3-node constant strain 2-D solid elements were used for both the web and flanges. This is a so-called "unfolded model", a modeling scheme frequently used to model a 3-D panel structure using 2-D solid elements. The finite element analyses were performed with the ISSAC computer code (Ref. 12).

The constitutive model for concrete in the ISSAC code is based on the concepts of orthotropic plasticity theory and the rotating smeared crack model, with a simplified biaxial envelope function as shown in Figure 7. For the compressive reduction factor of cracked concrete, the foregoing Equation 3 was used. The inelastic shear modulus is determined by modifying the foregoing Equation 5 as

$$G = \frac{1}{4(1+\nu)} (E_1 + E_2)/\sqrt{1 + (\epsilon_t/\epsilon_{cr})^2}$$

in which, ϵ_t is the tensile strain; and ϵ_{cr} is the cracking strain.

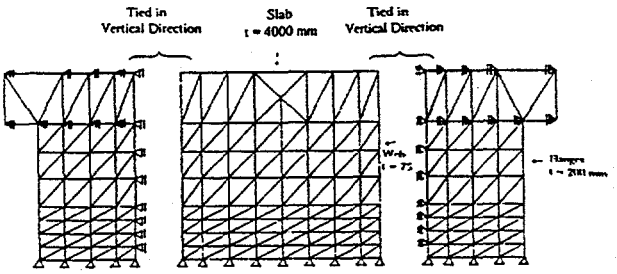

Figure 6 Finite Element Model

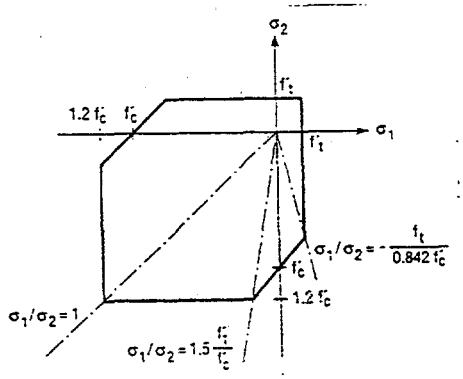

Figure 7 Biaxial Envelope Function

5 ANALYSIS RESULTS

Three types of analyses were performed by BNL, i.e., static monotonic (push-over), cyclic static and dynamic analyses. Figure 8 compares the push-over analysis results with recorded peak responses from six test runs. The parameter β is the ratio of the compressive strain at complete failure to that of the maximum strength. This parameter was assumed to be 10.0 in the following analyses. Figure 9 shows the predicted failure mode. It is obvious that the analysis predicted the wall to fail in sliding shear at the bottom of the web. The observed failure plane in the test (see Figure 4), however, is located approximately 40 cm from the bottom. One possible explanation for this difference may be the use of the plain-stress assumptions. An additional confinement due to large flanges may have shifted the location of failure. Almost identical failure patterns were also predicted in the following cyclic static and dynamic analyses.

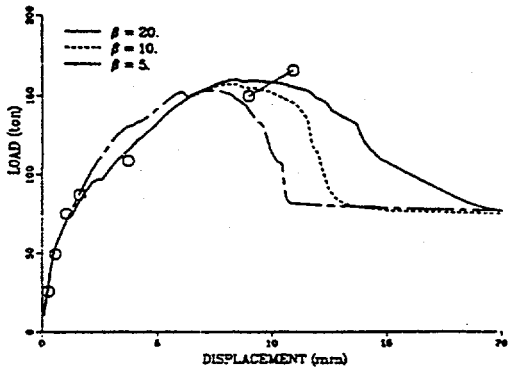

Figure 8 Load-Deformation Relationships from Push-over Analyses

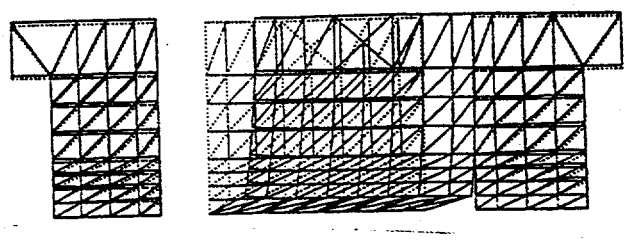

Figure 9 Predicted Sliding Shear Failure

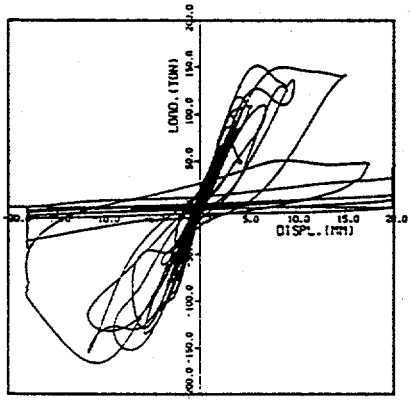

Figure 10 Load-Deformation Relationship from Test RUN-5

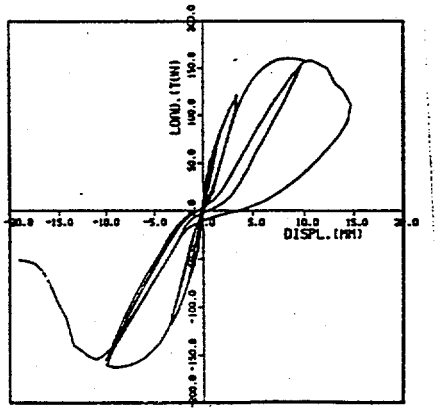

Figure 11 Load-Deformation Relationship from Cyclic Analysis

Figures 10 and 11 compares the load-deformation diagrams at the top slab obtained during the highest amplitude test of RUN-5 (Figure 10) and the calculated results under an idealized cyclic loading condition (Figure 11).

Relatively small hysteretic damping (i.e., hysteresis loop area), a significant pinching behavior, as well as sharp strength drop after reaching the maximum point, are observed both in the analysis and the test results. Those characteristics are considered to be consistent with the brittle sliding shear failure mode of the ISP wall. The maximum strength is 3% lower than that of the foregoing monotonic static analysis.

In the nonlinear dynamic analyses, the following Rayleigh damping was initially assumed:

$$[C] = \alpha [M] + \beta [K]$$

in which, [C], [M] and [K] are damping, mass and nonlinear stiffness matrices. Figures 12 and 13 compare the dynamic responses of the test and analysis for RUN-4. Although the overall predictions agree with the test results, high-frequency components were introduced numerically to the acceleration responses, adversely affecting the numerical stability.

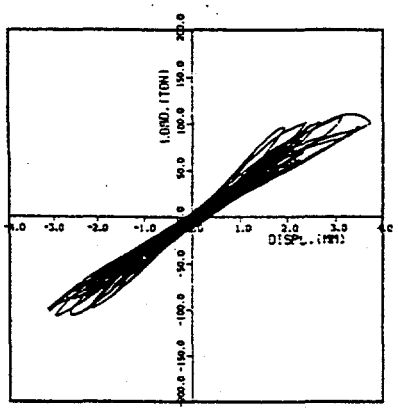

Figure 12 Load-Deformation Relationship from Test RUN-4

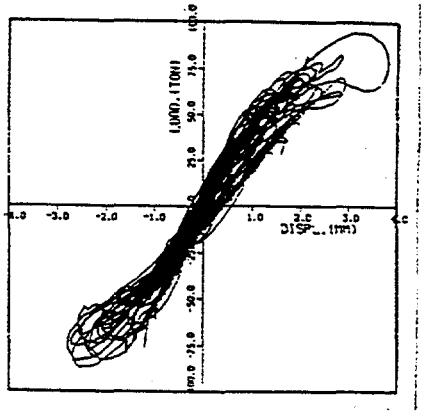

Figure 13 Load-Deformation Relationship from Initial Dynamic Analysis for RUN-4

In the improved analysis, the above Rayleigh damping was modified as,

$$[C] = \alpha [M] + \beta [K_e]$$

in which, $[K_e]$ is the elastic stiffness matrix. The newly performed dynamic analysis result is given in Figure 14. Although "a perfect match" between the analysis and test results was not achieved, it nevertheless improved the accuracy of the nonlinear FEM for the dynamic problem.

Figure 15 shows the predicted response for RUN-5. During the course of the analysis, a numerical difficulty was encountered as the analysis model was subjected to large plastic loading reversals. It was observed that as many elements started to crush and enter the negative slope region, the iterations using the initial stiffness method (see Figure 3(d)) tended to aggravate the solution. In the analysis, the iterations were turned off at t=2.5 sec. The analysis was terminated at t=3.616 sec., which coincides with the occurrence of the observed shear failure. Although some minor differences between the analysis predictions and the test results were observed between Figures 10 and 15, the analysis predicted the timing of sliding failure accurately.

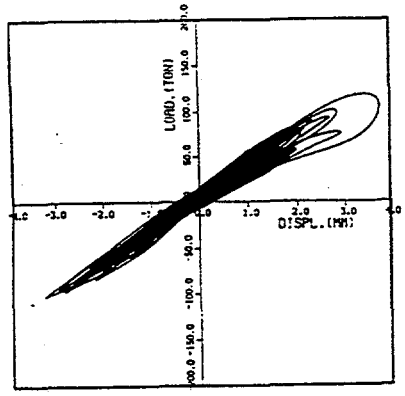

Figure 14 Load-Deformation Relationship from Improved Dynamic Analysis for RUN-4

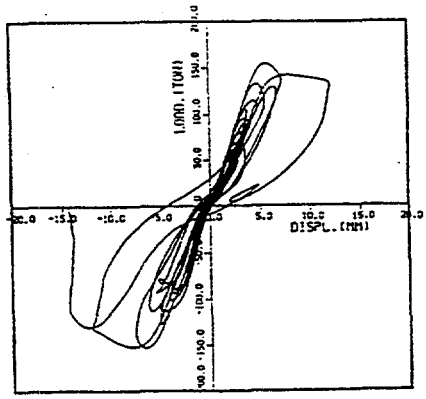

Figure 15 Load-Deformation Relationship from Dynamic Analysis for RUN-5

6 CONCLUSIONS

The SSWISP workshop provided a unique opportunity to review the reliability and applicability of various analysis methods to predict the dynamic behavior of shear wall structures under severe earthquake loads. The key elements of the nonlinear FEM analysis for concrete structures, i.e., the material constitutive models and numerical procedures, were reviewed based on the findings obtained during the SSWISP Workshop. The analysis results performed by BNL were also summarized. At the time of this writing, it appears that the applicability of nonlinear FEM analysis to full-size RC structures under severe earthquake loadings are still seriously limited. However, the reliability of analysis methods and the computational power of FEM codes seems to be improving rapidly in the last few years.

7 DISCLAIMER

This work was performed under the auspices of the U.S. Nuclear Regulatory Commission. The findings and opinions expressed in this paper are those of the authors, and do not necessarily reflect the views of the U.S. Nuclear Regulatory Commission or Brookhaven National Laboratory.

8 REFERENCES

1. Isenberg, J., Editor June 1991. Finite Element Analysis of Reinforced Concrete Structures II. Proceedings of International Workshop ASCE.
2. Nuclear Power Engineering Corporation, March 1996. Comparison Report, Seismic Shear Wall ISP, NUPEC's Seismic Ultimate Dynamic Response Test. NU-SSWISP-DO14, NUPEC.
3. Bažant, Z.P. & P.D. Bhat August 1976. Endochronic Theory of Inelasticity and Failure of Concrete. Journal of the Engineering Mechanics Division, ASCE, Vol. 102, No. EM4: pp. 701-722.
4. Liu, T.C.Y., et. al. May 1972. Biaxial Stress-Strain Relations for Concrete. Journal of the Structural Division, ASCE, Vol. 98, No. ST5: pp. 1025-1034.
5. Darwin, D. & D.A.W. Pecknold July 1974. Inelastic Model for Cyclic Biaxial Loading of Reinforced Concrete. University of Illinois at Urbana-Champaign, SRS No. 409.
6. Stevens, N.J., S.M. Uzumeri & M.P. Collins Jan. 1987. Analytical Modeling of Reinforced Concrete Subjected to Monotonic and Reversed Loadings. Department of Civil Engineering, University of Toronto, Publication No. F7-1.
7. Vecchio, F.J. & M.P. Collins December 1993. Compression Response of Cracked Reinforced Concrete. Journal of Structural Engineering, ASCE, Vol. 119, No. 12: pp. 3590-3610.
8. Hamada,S, M. Ohkubo & H. Noguchi October 1989. Basic Experiments on the Degradation of Cracked Concrete under Biaxial Compression and Tension. Annual Conference of AIJ: pp. 919-920.
9. Li, B., K. Maekawa, & H. Okamura 1989. Contact Density Model for Stress Transfer Across Cracks in Concrete. Journal of the Faculty of Engineering, The University of Tokyo, Vol. XXX, No. 1: pp. 9-52.
10. Kinugasa, H., et. al. October 1989. Stress Transfer Model for Cracked Concrete under Cyclic Loading. Annual Meeting of Architectural Institute of Japan: pp. 925-926.

11. Matzen, V.C., et. al. December 1994. Improved Finite Element Analysis to Simulate Ratcheting in Piping. Current Issues Related to Nuclear Power Plant Structures, Equipment and Piping, Orlando, Florida.
12. Park, Y.J. February 1995. ISSAC, User's Manual," Informal Report. Brookhaven National Laboratory.